

EFFECT OF ROTOR ECCENTRICITY ON MAGNETIC NOISE GENERATION IN INDUCTION MOTORS

A. REZIG M. R. MEKIDECHE

LAMEL Laboratory Jijel University
Electrical Engineering Department, Jijel University, Algeria, alirezikdz@yahoo.fr mek_moh@yahoo.fr

N. IKHLEF

LAMEL Laboratory Jijel University
Electrical Engineering Department, Jijel University, Algeria, ikhfabil@yahoo.fr

Abstract: This paper presents an analytical approach to modelling radial magnetic force acting on stator surface of induction motors, this model covering the most important causes of magnetic noise such as saturation, eccentricity, slots and winding distribution. The study of magnetic noise due to eccentricity is given, which demonstrate the adverse effect of this phenomena, often occurring due to production inaccuracies.

Key words: magnetic noise, eccentricity, permeance, magnetomotive force, radial force, modes, natural frequency.

1. Introduction

The majority of electric machines function at variable speed which generally induces noise and vibration for speed or a given frequency. For manufacturing industries but also with the growing number of international regulatory institutions that aimed at controlling noise emission of electric machines bares testimony to the seriousness of this problem [1,2]. The sources of this phenomena are multiples there are mechanical sources, aerodynamic sources and electromagnetic sources which are considered here, and result from the action of magnetic forces in the air gap[8]. Magnetic forces in motors consist of three main kinds; tangential forces which act on the rotor to produce torque, radial forces which are attractive forces between the stator and the rotor, and magnetostrictive forces which act to stretch the iron in the same direction as the magnetic field. Radial magnetic forces are by far the main cause of magnetic noise in induction machines [7]. A classical method to study magnetic noise is the finite elements method (FEM) in magneto-dynamics, including coupling circuit. However, in the case of strong coupling, taking into account the electromagnetic and vibro-acoustic models at the same time would need a considerable computing time [2]. In order to solve this problem, an analytical approach is considered instead, taking into account the most important causes of magnetic noise, i.e. saturation, slots, winding distribution and eccentricity. A study of magnetic noise due to eccentricity is given, which demonstrate the adverse

effect of this phenomena, often occurring due to manufacturing faults.

2. Magnetic model

In this work, it is assumed that the iron is infinitely permeable in relation to the air, so that the air gap radial magnetic force per unit area can be calculated using the following Maxwell's equation for stress tensor [5,6]:

$$\sigma = \frac{B^2(\theta, t)}{2\mu_0} \quad (1)$$

Where B is the air gap magnetic flux density, μ_0 is the permeability of free space, θ is angular coordinate (in radians) around the circumference, and t the time. The flux density is approximated by the product between the air gap permeance and magnetomotive force:

$$B(\theta, t) = \Lambda(\theta, t)F(\theta, t) \quad (2)$$

Where Λ is the air gap permeance, and F is the magnetomotive force. Both Λ and F are expressed as series of space harmonics to take into account the generally no uniform air gap and the no sinusoidal distribution of winding bars.

3. Air gap permeance

The effective air gap permeance is modelled as a sum of constant part and harmonic components caused by slots, eccentricity, and saturation. The resultant permeance per unit area can be written as

$$\Lambda(\theta, t) = \frac{\mu_0}{\delta_{sl} + \delta_{ec}(\theta, t) + \delta_{sat}(\theta, t)} \quad (3)$$

Where δ_{sl} is the effective air gap when considering the stator and rotor slots, δ_{ec} is the change in the air gap due to eccentricity, while δ_{sat} is fictitious increase in the air gap that accounts for saturation of the teeth tips [1].

The presence of slots on the stator and rotor causes the average air gap to be slightly larger. This air gap can therefore be expressed as follows

$$\delta_{sl}(\theta, t) = \delta_0 + \delta_1(\theta, t) + \delta_2(\theta, t) \quad (4)$$

Where δ_0 is the nominal air gap, δ_1 and δ_2 are the changes in the air gap length, due to slots on the stator and the rotor respectively. The effective air gap in (4) can be determined by using Fourier series, whose coefficients are calculated from the slots geometry [1]. Consider a smooth rotor of radius r , eccentrically supported inside a smooth stator with radius R , as shown in Fig.1. From Fig.1 we note that the air gap length becomes a function of the angular displacement θ and time t , given by

$$\begin{aligned}\delta_{ec}(\theta, t) &= R - r - e \cos(\theta - w_\epsilon t - \varphi_\epsilon) \\ &= \delta_0 \{1 - \epsilon \cos(\theta - w_\epsilon t - \varphi_\epsilon)\}\end{aligned}\quad (5)$$

Where $\delta_0 = R - r$, ϵ is referred to as the relative eccentricity $\epsilon = e/\delta_0$, w_ϵ is the angular frequency in relation to the stator ($w_\epsilon = 0$ for static eccentricity, $w_\epsilon = w/p$ for dynamic eccentricity), and φ_ϵ is the phase angle

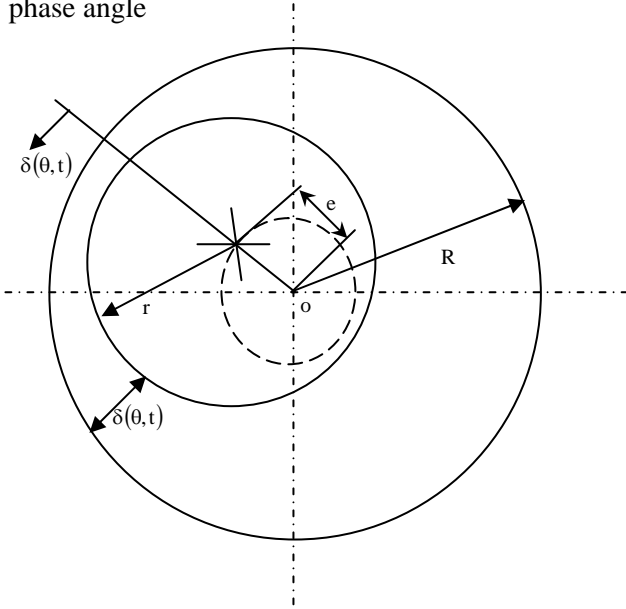


Fig. 1. An eccentric rotor in a smooth air gap.

The increase in air gap can be expressed as follows

$$\delta_{sat}(\theta, t) = \delta_s [1 + \cos 2(p\theta - wt - \varphi_s)] \quad (6)$$

Where the constant δ_s is governed by the relationship between the magnetisation of the teeth, back iron and the air [2].

The resultant permeance is obtained by substituting equation (5), (6), and (6) into equation (3), giving the equation

$$\Lambda(\theta, t) = \frac{\mu_0}{\delta_0 \left[1 + \frac{1}{\delta_0} (\delta_{sl}(\theta, t) + \delta_{ec}(\theta, t) + \delta_{sat}(\theta, t)) \right]} \quad (7)$$

The expression in (7) can be expanded and simplified into the form [8].

$$\Lambda(\theta, t) = \Lambda_0 - \Lambda_1(\theta, t) - \Lambda_2(\theta, t) - \Lambda_\epsilon(\theta, t) - \Lambda_{sat}(\theta, t) \quad (8)$$

Where Λ_0 is the mean air gap permeance, Λ_1 , Λ_2 , Λ_ϵ , and Λ_{sat} are the harmonics due to stator and rotor slots, eccentricity, respectively.

4. Magnetomotive force harmonics

The flow of currents in the stator and the rotor winding of an induction machine produces series of *mmf* harmonics across the air gap, in addition to the fundamental. The resultant air gap magnetomotive force is a sum of the two *mmfs*. The shape and magnitude of this *mmf* depends on many parameters, including the number of phases of the winding, the number and shape of the slots, the spatial arrangement of the winding, pole-pitch and rotor skew. The analysis of the total *mmf* can be found in [1, 4]. Nevertheless, the total *mmf* can be expressed as a sum of the stator *mmf* and the rotor *mmf* in the following general form:

$$F(\theta, t) = F_p(\theta, t) + F_1(\theta, t) + F_{2,1}(\theta, t) + F_{2,2}(\theta, t) \quad (9)$$

Where F_p is the fundamental stator *mmf* wave, F_1 represent the stator *mmf* harmonics, $F_{2,1}$ represent the rotor *mmf* produced by the rotor fundamental current, and $F_{2,2}$ represents the rotor *mmf* produced by rotor current harmonics.

5. Air gap flux density waves

The air gap flux density is calculated from the product of the permeance and the magnetomotive force waves as given in equation (2). After substituting the expression for the permeance and magnetomotive force derived in paragraph 3 and 4, into equation (2), the total air gap field can be written as

$$\begin{aligned}B(\theta, t) &= F(\theta, t) \Lambda(\theta, t) \\ &= [F_p(\theta, t) + F_1(\theta, t) + F_{2,1}(\theta, t) + F_{2,2}(\theta, t)] \times \\ &\quad [\Lambda_0 + \Lambda_1(\theta, t) + \Lambda_2(\theta, t) + \Lambda_{1,2}(\theta, t) + \Lambda_\epsilon(\theta, t) - \Lambda_{sat}(\theta, t)]\end{aligned}\quad (10)$$

Carrying out the entire product in equation (10), term by term is computationally demanding and inefficient. In as far magnetic noise is concerned, it is sufficient to consider only the products that result in most important flux density waves. According to [3, 7], the following flux density waves are the most significant for noise analysis.

- Fundamental air gap flux density,
- Stator winding harmonics,
- Rotor winding harmonics,
- Stator slots harmonics,
- Rotor slots harmonics,
- Saturation harmonics, and
- Eccentricity harmonics.

5.1 Fundamental air gap flux density

The fundamental air gap flux density wave is obtained by multiplying the mean air gap permeance and *mmf* wave waves.

$$b_p(\theta, t) = \Lambda_0 F_p(\theta, t) = B_p \cos(p\theta - w_1 t - \varphi_m) \quad (11)$$

Where p is number of pole-pairs, w_1 is the fundamental frequency, φ_m is the phase angle of no load current.

5.2 Stator winding harmonics

Stator winding flux density wave are calculated from the mean air gap permeance and the stator mmf harmonics, using the following expression

$$b_{sw} = \Lambda_0 F_1(\theta, t) = \sum_v B_{sw,v} \cos(vp\theta - w_v t - \varphi_v) \quad (12)$$

Where

$$v = 6k + 1; k = \pm 1, \pm 2, \pm 3, \dots$$

$$w_v = w_1 \quad (13)$$

$$\varphi_v = \varphi_m$$

5.3 Rotor winding harmonics

These flux density harmonics are a result of the interaction between the rotor mmf, $F_{2,1}$ and the constant term of the air gap permeance according to the following equation

$$b_{rw}(\theta, t) = \Lambda_0 F_{2,1}(\theta, t) = \sum_\mu B_{rw,\mu} \cos(\mu p\theta - w_\mu t - \varphi_\mu) \quad (14)$$

Where

$$\mu = kQ_r + p, \quad k = 0, \pm 1, \pm 2, \pm 3, \dots$$

$$w_\mu = w_1 \left[1 + \frac{kQ_r}{p} (1-s) \right] \quad (15)$$

Where Q_r the number of rotor slots, s the fundamental slip and φ_μ the phase angle of the rotor harmonics current.

5.4 Stator slots harmonics

Stator slots harmonics are generated by the interaction between the fundamental mmf wave, and the stator partial permeance wave, Λ_1 .

$$b_{ss}(\theta, t) = A_1(\theta) * F_p(\theta, t) = \sum_v B_{ss,v} \cos(vp\theta - w_1 t - \varphi_v) \quad (16)$$

Where

$$v = kQ_s + p, \quad k = \pm 1, \pm 2, \pm 3, \dots \quad (17)$$

$$\varphi_v = \varphi_m$$

Q_s the number of stator slots.

From the equations (16) and (17) we note that the stator slot harmonics have pole-pair equal to $v = Q_s \pm p, 2Q_s \pm p, 3Q_s \pm p, \dots$ and have the same angular frequency as the fundamental wave.

5.5 Rotor slots harmonics

The slots harmonics are defined here as the air gap flux density generated by the rotor slots and the fundamental stator mmf field.

$$b_{rs}(\theta, t) = \Lambda_2(\theta, t) * F_p(\theta, t)$$

$$= \sum_v B_{rs,v} (vp\theta - w_v t - \varphi_v) \quad (18)$$

Where

$$v = kQ_r + p, \quad k = \pm 1, \pm 2, \pm 3, \dots$$

$$w_v = w_1 \left[1 + k \frac{Q_s}{p} (1-s) \right] \quad (19)$$

$$\varphi_v = \varphi_m$$

From the equation (18) and (19) it is noted that stator slot harmonics have pole-pair numbers which depend on the stator slots, given by $v = Q_r \pm p, 2Q_r \pm p, 3Q_r \pm p, \dots$. In contrast to the stator slot harmonics, rotor slots harmonics have angular frequency that are functions of the fundamental slip.

5.6 Saturation harmonics

Saturation flux density harmonics are defined here as those harmonics that are generated from the interaction between the air gap permeance saturation harmonics and the fundamental stator field.

$$b_{sat}(\theta, t) = -\Lambda_{sat}(\theta, t) F_p(\theta, t) \quad (20)$$

$= -B_{sat} [\cos(p\theta - w_1 t - \varphi_m) + \cos(3p\theta - 3w_1 t - 3\varphi_m)]$
In line with the fact that each air gap flux density wave induces corresponding rotor harmonic current, one must take into account additional air gap rotor residual fields generated by the saturation flux density wave [1].

5.7 Eccentricity harmonics

The eccentricity flux density waves are generated by the interaction between the eccentricity permeance waves and the fundamental mmf field. Among the eccentricity permeance wave, usually only the first harmonic is important both in terms of magnitude and from noise generation point of view. If the first eccentricity permeance harmonic is multiplied with the fundamental mmf we obtained the following equation

$$b_e(\theta, t) = \left[\frac{\varepsilon \mu_0}{\delta_0 (k_{c1} k_{c2})^2} \cos(\theta - w_\varepsilon t - \varphi_\varepsilon) \right] F_p(\theta, t) \quad (21)$$

$$= B_p \frac{e}{2\delta_0 k_{c1} k_{c2}} \cos(v_\varepsilon \theta - w'_\varepsilon t - \varphi'_\varepsilon)$$

Where

$$v_\varepsilon = p \pm 1$$

$$w'_\varepsilon = w_1 \pm w_\varepsilon$$

$$\varphi'_\varepsilon = \varphi_m \pm \varphi_\varepsilon \quad (22)$$

$$w_\varepsilon = \begin{cases} 0 & \text{for static eccentricity} \\ \frac{w_1}{p} (1-s) & \text{for dynamic eccentricity} \end{cases}$$

From equation (22) it is noted that eccentricity flux

density harmonics have pole-pairs equal to $p \pm 1$

The eccentricity flux density waves generate also some residual rotor flux density waves.

6. Radial magnetic forces waves

The radial magnetic forces are calculated using the Maxwell stress method [5,6]. In order to facilitate the analysis, we separate the air gap flux density terms obtained in section (5) are grouped according to their sources, i.e. according to whether the flux density wave originates from the stator or from the rotor, as shown in the following equation:

$$B(\theta, t) = b_p(\theta, t) + \sum_v b_v(\theta, t) + \sum_\mu b_\mu(\theta, t) \quad (23)$$

Where the script p represents the fundamental component of stator field, v represents flux density harmonic terms originating from the stator (including the saturation and eccentricity terms), and μ , represents flux density harmonic terms originating from the rotor.

The force equation can be written as follows:

$$\sigma(\theta, t) = \frac{B^2(\theta, t)}{2\mu_0} = \frac{1}{2\mu_0} \left\{ b_p^2 + 2 \left[\sum_v b_p b_v + \sum_\mu b_p b_\mu + \sum_{\mu\nu} b_v b_\mu \right] + 2 \left[\sum_{v_1 \neq v_2} b_{v_1} b_{v_2} + \sum_{\mu_1 \neq \mu_2} b_{\mu_1} b_{\mu_2} \right] + \sum_v b_v^2 + \sum_\mu b_\mu^2 \right\} \quad (24)$$

Each product between any two flux density waves in the previous equation produce two radial magnetic forces revolving in opposite directions along the air gap. Each component of the product, i.e. each force wave, can be written in following general form

$$\sigma_r(\theta, t) = \hat{\sigma}_r(\theta, t) \cos(r\theta - w_r t - \phi_r) \quad (25)$$

Where $\hat{\sigma}_r$ is the amplitude of radial force, r is the mode number, w_r is the angular frequency, and ϕ_r is phase angle. Because of the large number of terms involved in implementing equation (25), and because some terms have no value for magnetic noise, it is necessary to select only the relevant forces.

The following criteria are used to identify the potential noise generation forces:

a- Force wave with low mode number should be considered important, since the noise radiation efficiency decrease with increase in mode number. Mode number $r=1, 2, 3, 4$ are particularly important for small size induction motors [1], [8].

b- Only frequencies within the range 100 Hz-4000Hz are significant for generation of magnetic noise. Using equation (25) the following can be summarised (assuming a 50 Hz supply):

- The square of fundamental flux density wave gives magnetic force components in the frequency range 0 to

100 Hz, which is not important for noise, providing there is not mechanical resonance.

- The square terms, compressing stator fields and rotor fields gives forces that generally have high mode numbers, and are therefore less significant, unless there is mechanical resonance. An exception to this is the eccentricity component (b_{ecc}^2) that has very important mode numbers in the range 0, $2, 2p$, and $2p+1$.

- The most important category seems to be contained by the second term in the parentheses of equation (25). For example the product between the fundamental field and eccentricity field gives force modes in the range $r=1, 2p-1, 2p+1$.

A complete analysis can only be made by simulation, taking into account mode numbers and frequency range, but the size of the forces amplitudes as well as mechanical properties of the machines.

7. Simulations and results

The subjects of this section are as follows:

- Implementation of the analytical model in predicting the radial magnetic forces.

- To demonstrate the effect of rotor static eccentricity on the acoustic noise by creation of mode vibration 1, 2, 3...

For this purpose four simulations were made, based on the induction motor specified in table.1. In the first two simulations, the rotor eccentricity was set at 0%, while the motor speed was set at the rated load value of 1459 rpm, in one case and then at no load speed in the other case.

Description	value
Rated power, kW	15
Number of phases	03
Rated frequency, Hz	50
Rated voltage, V	380
Number of stator slots	36
Number of rotor slots	28
Air gap length, mm	0.4

Table. 1. Parameters specification of motor used in simulation

In the other two simulations, the rotor eccentricity was set at 25%, while the motor speed was first set at the rated value of 1459 rpm, and then at the synchronous of 1500 rpm in the other simulation. The rated voltage was 380 V, and stator current on load was equal to 29.8 A, while the current at no load was equal to 11.5 A. The simulation results are presented below.

In figures (2) and (3) we show the spectra of the radial magnetic force on no load and on load with a static eccentricity of 0%. It is noted that for a 0% eccentricity only modes 0 and 4 are present. The most dominant force in both figures is mode 4 force at 100 Hz. This is caused by the fundamental flux density

component. The natural frequencies corresponding to mode 0 and 4 are considerably high in this motor (about 5 kHz and 6 kHz respectively). The most important modes are modes 1, 2, and 3.

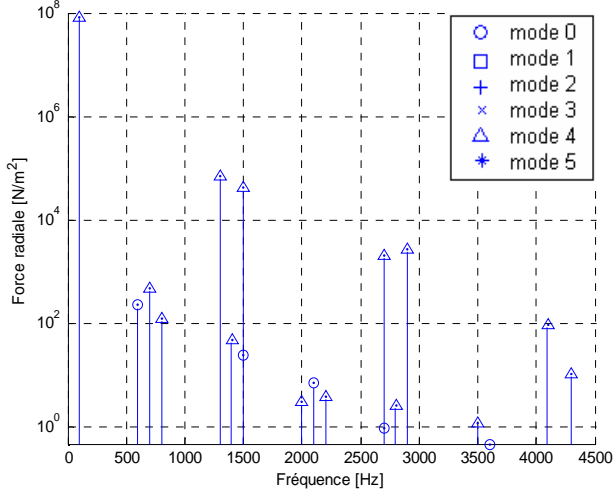


Fig. 2. Radial magnetic force spectra on stator with 0% eccentricity at no load (1500 rpm)

include modes 1, 2, 3 and 5 due to eccentricity. There is one mode 2 radial force, at frequency of 800 for the 1500 rpm motor speed, and at 780 Hz, for the 1459 rpm speed, this mode (mode2) is very important for this motor because the stator natural frequency calculated for this motor is about 1 kHz.

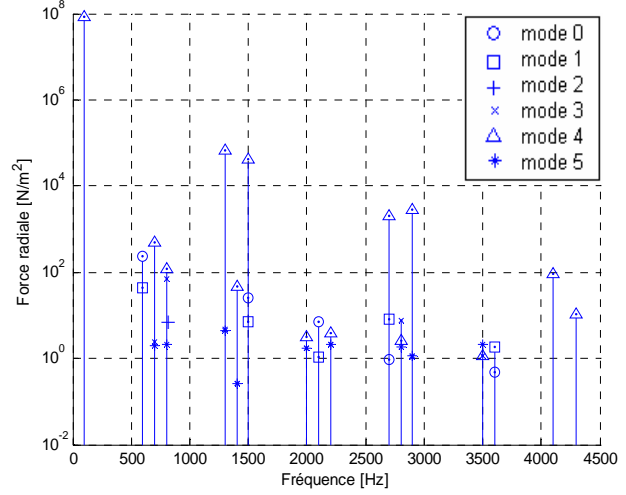


Fig. 4. Radial magnetic force spectra on stator with 25% eccentricity at no load (1500 rpm)

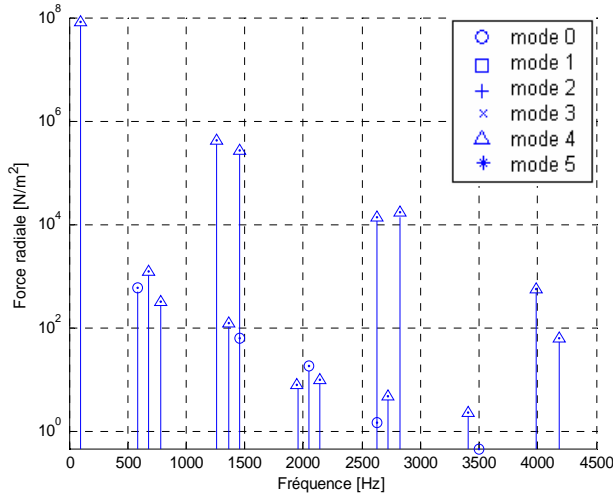


Fig. 3. Radial magnetic force spectra on stator with 0% eccentricity at load (1459 rpm)

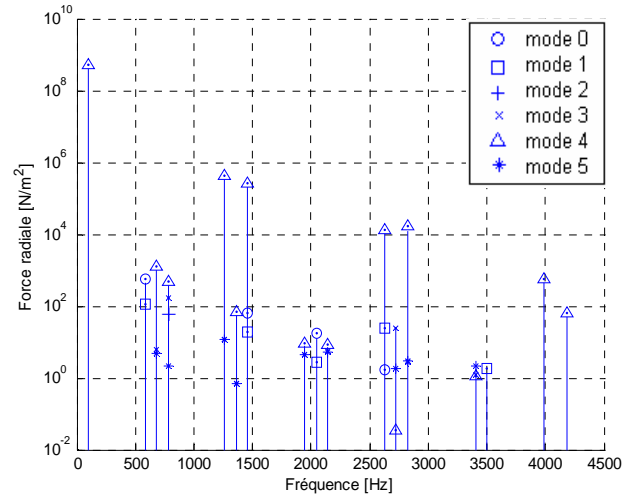


Fig. 5. Radial magnetic force spectra on stator with 0% eccentricity at load (1459 rpm)

The magnetic force spectra for 25% static rotor eccentricity are shown in figures (4) and (5), for speeds of 1500 rpm and 1459 rpm, respectively. One noticeable feature from the figures when compared to previous figures is that some additional forces have been introduced in the spectrum. The new forces

8. Conclusion

This paper presented the simulation of radial magnetic forces. The aim was to demonstrate the effectiveness of the analytical model to isolate the different noise phenomena. In this case, was on the static eccentricity. However, the method can be used to

study the influence of other phenomena such as saturation, slots, and the winding arrangement. The results confirm the effect of eccentricity in generating low-mode radial forces. It was shown that for the motor used in this simulation, there were no low mode forces unless when eccentricity occurs. This particularity is important for manufacturing and assembly of motors, because it is shown that even though a motor is designed carefully for low noise, if the manufacturing and assembly process is not conducted properly to minimise eccentricity, the motor could be noisy.

References

1. Gieras, J.F., Wang, C., Lai, J.C.: *Noise in polyphase electric motors*. Taylor & Francis edition, 2006.
2. Maliti, K.C.: *Modelling and Analysis of Magnetic Noise in Squirrel Cage Induction Motors*. Doctoral dissertation royal institute of technology, Stockholm, 2000.
3. Timar, P.L.: *Noise and Vibration of Electrical Machines*. Budapest Akademiai Kiado, 1989.
4. Alger, P.L.: *The Nature of Induction Machines*. Gordon and Breach, New York, 1965.
5. Coulomb, J. L.: *A methodology for determination of global electromechanical quantities from a finite analysis and its application to the evaluation of magnetic forces, torque and stiffness*. In: IEEE trans on .magn, vol.19, No.6, Nov 1983, p. 2514-2519.
6. Rezig, A., Ikhlef, N., Mékidèche, M.R.: *Electromagnetic Force Calculation from Finite Element field Solutions*. In: 7th International Symposium on Electric and Magnetic Fields EMF, June 19-22, 2006, Aussois, France.
7. Yacamini, R., Chang, S.C.: *Noise and vibration from Induction Machines fed from Harmonic Source*. In: IEEE Tran on energy conversion, vol.10, No.2, June 1995.
8. Nau, S.L., Mello, H.G.: *Acoustic Noise in Induction Motors: Causes and Solutions*, IEEE 2000